



Modeling and simulation of online reprocessing in the thorium-fueled molten salt breeder reactor

Andrei Rykhlevskii, Jin Whan Bae, Kathryn D. Huff*

Dept. of Nuclear, Plasma, and Radiological Engineering, University of Illinois at Urbana-Champaign, Urbana, IL 61801, United States



ARTICLE INFO

Article history:

Received 12 September 2018
Received in revised form 5 January 2019
Accepted 17 January 2019
Available online 25 January 2019

Keywords:

Molten salt reactor
Molten salt breeder reactor
Python
Depletion
Online reprocessing
Nuclear fuel cycle
Salt treatment

ABSTRACT

In the search for new ways to generate carbon-free, reliable base-load power, interest in advanced nuclear energy technologies, particularly Molten Salt Reactors (MSRs), has resurfaced with multiple new companies pursuing MSR commercialization. To further develop these MSR concepts, researchers need simulation tools for analyzing liquid-fueled MSR depletion and fuel processing. However, most contemporary nuclear reactor physics software is unable to perform high-fidelity full-core depletion calculations for a reactor design with online reprocessing. This paper introduces a Python package, SaltProc, which couples with the Monte Carlo code, SERPENT2 to simulate MSR online reprocessing by modeling the changing isotopic composition of MSR fuel salt. This work demonstrates SaltProc capabilities for a full-core, high-fidelity model of the commercial Molten Salt Breeder Reactor (MSBR) concept and verifies these results to results in the literature from independent, lower-fidelity analyses.

© 2019 Elsevier Ltd. All rights reserved.

1. Introduction

The MSR is an advanced nuclear reactor developed at Oak Ridge National Laboratory (ORNL) in the 1950s and operated in the 1960s. More recently, the Generation IV International Forum (GIF) included MSRs among the six most promising advanced reactor concepts for further research and development. MSRs offer significant improvements “in the four broad areas of sustainability, economics, safety and reliability, and proliferation resistance and physical protection” (U.S. DoE, 2002). To achieve the goals formulated by the GIF, MSRs attempt to simplify the reactor core and improve inherent safety by using liquid fuel.

In the thermal spectrum MSR, fluorides of fissile and/or fertile materials (i.e. UF_4 , ThF_4 , PuF_3 , TRU^1F_3) combine with carrier salts to form a liquid fuel that circulates in a loop-type primary circuit (Haubenreich and Engel, 1970). Immediate advantages over traditional commercial reactors include near-atmospheric pressure in the primary loop, relatively high coolant temperature, outstanding neutron economy, and improved safety parameters. Advantages over solid-fueled reactors in general include reduced fuel preprocessing and the ability to continuously remove fission products and add fissile and/or fertile elements (LeBlanc, 2010).

The thorium-fueled MSBR was developed in the early 1970s by ORNL specifically to explore the promise of the thorium fuel cycle, which uses natural thorium instead of enriched uranium. With continuous fuel reprocessing, the MSBR realizes the advantages of the thorium fuel cycle because the ^{233}U bred from ^{232}Th is almost instantly² recycled back into the core (Betzler et al., 2016). The chosen fuel salt, $\text{LiF}-\text{BeF}_2-\text{ThF}_4-\text{UF}_4$, has a melting point of 499°C, a low vapor pressure at operating temperatures, and good flow and heat transfer properties (Robertson, 1971). Finally, the MSR also could be employed as a converter reactor for transmutation of spent fuel from current Light Water Reactor (LWR).

Liquid-fueled systems present a challenge to existing neutron transport and depletion tools, which are typically designed to simulate solid-fueled reactors. To handle the material flows and potential online removal and feed of liquid-fueled systems, early MSR simulation methods at ORNL integrated neutronics and fuel cycle codes (i.e., Reactor Optimum Design (ROD) (Bauman et al., 1971)) into operational plant tools (i.e., Multiregion Processing Plant (MRPP) (Kee and McNeese, 1976)) for MSR and reprocessing system design. Based on this approach, recent tools from universities and research institutions can approximate online refueling (Serp et al., 2014). A summary of recent efforts is listed in Table 1.

* Corresponding author.

E-mail address: kdhuff@illinois.edu (K.D. Huff).

¹ Transuranic elements.

² ^{232}Th transmuted into ^{233}Th after capturing a neutron. Next, this isotope decays to ^{233}Pa ($\tau_{1/2} = 21.83$ m), which finally decays to ^{233}U ($\tau_{1/2} = 26.967$ d).

Table 1

Tools and methods for MSRs fuel cycle analysis.

Neutronic code	Authors	Spectrum
MCNP/REM (MCNP, 2004; Heuer et al., 2010)	Doligez et al. (2014) and Heuer et al. (2014)	Fast
ERANOS (Ruggieri et al., 2006)	Fiorina et al. (2013)	Fast
KENO-IV/ORIGEN (Goluoglu et al., 2011; Gauld et al., 2011)	Sheu et al. (2013)	Fast
SERPENT2 Leppanen et al., 2015	Aufiero et al. (2013) and Ashraf et al. (2018)	Fast
DIF3D (Derstine, 1984)	Zhou et al. (2018)	Thermal/fast
MCODE/ORIGEN2 (Xu and Hejzlar, 2008; Croff, 1980)	Ahmad et al. (2015)	Thermal
MCNP6/CINDER90 (Goorley et al., 2013)	Park et al. (2015) and Jeong et al. (2016)	Thermal
SCALE/TRITON (Bowman, 2011; Powers et al., 2013)	Powers et al. (2013), Powers et al. (2014) and Betzler et al. (2017a)	Thermal/fast
SERPENT2	Rykhlevskii et al. (2017a)	Thermal
MCNP/REM	Nuttin et al. (2005)	Thermal

Doligez et al. (2014), Heuer et al. (2014), Sheu et al. (2013) and Aufiero et al. (2013) simulate some form of reactivity control, and methods (Doligez et al., 2014; Heuer et al., 2014; Aufiero et al., 2013; Ahmad et al., 2015; Park et al., 2015; Jeong et al., 2016; Rykhlevskii et al., 2017a; Nuttin et al., 2005) use a set of all nuclides in depletion calculations.

Many liquid-fueled MSR designs rely on online fuel processing in which material moves to and from the core continuously or at specific time steps (batch-wise). In the batch-wise approach, the burn-up simulation stops at a given time and restarts with a new liquid fuel composition (after removal of discarded materials and addition of fissile/fertile materials). ORNL researchers have developed ChemTriton, a Python-based script for SCALE/TRITON which uses the batch-wise approach to simulate a continuous reprocessing and refill for either single or multiple fluid designs. ChemTriton models salt treatment, separations, discharge, and refill using a unit-cell MSR SCALE/TRITON depletion simulation over small time steps to simulate continuous reprocessing and deplete the fuel salt (Powers et al., 2013). Methods listed in Zhou et al. (2018), Sheu et al. (2013), Park et al. (2015), Jeong et al. (2016), Powers et al. (2014), Betzler et al. (2017a) and Rykhlevskii et al. (2017a) as well as the current work also employ a batch-wise approach.

Accounting for continuous removal or addition presents a greater challenge since it requires adding a term to the Bateman equations. Fiorina et al. simulated Molten Salt Fast Reactor (MSFR) depletion with continuous fuel salt reprocessing via introducing “reprocessing” time constants into the ERANOS transport code (Fiorina et al., 2013). The latest SCALE release will also have the same functionality using truly continuous removals (Betzler et al., 2017b). A similar approach is adopted to model true continuous feeds and removals using the MCNP transport code listed in Doligez et al. (2014), Heuer et al. (2014) and Nuttin et al. (2005).

Thorium-fueled MSBR-like reactors similar to the one in this work are described in Park et al. (2015), Jeong et al. (2016), Powers et al. (2013), Powers et al. (2014), Betzler et al. (2017a), Rykhlevskii et al. (2017a) and Nuttin et al. (2005). Nevertheless, most of these efforts considered only simplified unit-cell geometry because depletion computations for a many-year fuel cycle are computationally expensive even for simple models.

Nuttin et al. broke up the reactor core geometry into three Monte Carlo N-Particle code (MCNP) cells: one for salt channels, one for the salt plena above and below the core, and a third cell for the annulus. Consequently, the two-region reactor core was approximated by one region with averaged fuel/moderator ratio

(Nuttin et al., 2005). Powers et al., Betzler et al., and Jeong et al. (Powers et al., 2013; Powers et al., 2014; Betzler et al., 2016; Betzler et al., 2017a; Jeong et al., 2014; Jeong et al., 2016) used a similar approach. This approach misrepresents the two-region breeder reactor concept. The unit-cell or one-region models may produce reliable results for homogeneous reactor cores (i.e. MSFR, Molten Salt Actinide Recycler and Transmuter (MOSART)) or for one-region single-fluid reactor designs (i.e. Molten Salt Reactor Experiment (MSRE)). However, a two-region MSBR must be simulated using a whole-core model to capture different neutron transport characteristics in the inner and outer regions of the core. In particular, most fissions happen in the inner region while breeding occurs in the outer zone.

Aufiero et al. added an undocumented feature to SERPENT2 using a similar methodology by explicitly introducing continuous reprocessing in the system of Bateman equations and adding effective decay and transmutation terms for each nuclide (Aufiero et al., 2013). This was employed to study the material isotopic evolution of the MSFR (Aufiero et al., 2013). The developed extension directly accounts for the effects of online fuel reprocessing on depletion calculations and features a reactivity control algorithm. The extended version of SERPENT2 was assessed against a dedicated version of the deterministic ERANOS-based EQL3D procedure in Ruggieri et al. (2006) and Fiorina et al. (2013) and adopted to analyze the MSFR fuel salt isotopic evolution.

We employed this built-in SERPENT2 feature for a simplified unit-cell geometry of the thermal spectrum thorium-fueled MSBR and found it unusable³. Primarily, it is undocumented, and the discussion forum for SERPENT users is the only useful source of information at the moment. Additionally, the reactivity control module described in Aufiero et al. is not available in the latest SERPENT 2.1.30 release. Third, the infinite multiplication factor behavior for simplified unit-cell model obtained using SERPENT2 built-in capabilities (Rykhlevskii et al., 2017a) does not match with exist MCNP6/Python-script results for the similar model by Jeong and Park⁴ (Jeong et al., 2016).

If these challenges can be overcome through verification against ChemTriton/SCALE as well as this work (the SaltProc/SERPENT2 package), we hope to employ this SERPENT2 feature for removal of fission products with shorter residence time (e.g., Xe, Kr), since these have a strong negative impact on core lifetime and breeding efficiency.

The present work introduces the online reprocessing simulation package, SaltProc, which expands the capability of the continuous-energy Monte Carlo Burnup calculation code, SERPENT2 (Leppanen et al., 2015), for simulation liquid-fueled MSR operation (Rykhlevskii et al., 2018). It also reports the application of the coupled SaltProc-SERPENT2 system to the MSBR, an extension of the work presented Rykhlevskii et al. (2017b) and Rykhlevskii et al. (2017a). In this work, we analyzed MSBR neutronics and fuel cycle to establish its equilibrium core composition. Additionally, we compared predicted operational and safety parameters of the MSBR at both the initial and equilibrium states to characterize the evolution of its safety case over time. Finally, these simulations determined the appropriate ²³²Th feed rate for maintaining criticality and enabled analysis of the overall MSBR fuel cycle performance.

The works described in Park et al. (2015) and Jeong et al., 2016 are most similar to the work presented in this paper. However, a

³ Some challenges in no particular order: mass conservation is hard to achieve; three types of mflow cards (0, 1 or 2) are indistinguishable in purpose; an unexplained difference between CRAM and TTA results; etc.

⁴ In our study k_{∞} drops from 1.05 to 1.005 during a 1200 days of depletion simulation while in Jeong and Park work this parameter decreasing slowly from 1.065 to 1.05 for the similar time-frame.

few major differences follow: (1) Park et al. employed MCNP6 for depletion simulations while this work used SERPENT2; (2) the full-core reactor geometry herein is more detailed (Rykhlevskii et al., 2017b); (3) Park et al. and Jeong et al. both only considered volatile gas removal, noble metal removal, and ^{233}Pa separation while the current work implemented the more detailed reprocessing scheme specified in the conceptual MSBR design (Robertson, 1971); (4) the ^{232}Th neutron capture reaction rate has been investigated to prove advantages of two-region core design; (5) the current work explicitly examines the independent impacts of removing specific fission product groups.

The complex MSBR geometry is challenging to describe in software input, and usually researchers make significant geometric simplifications to model it (Park et al., 2015). This study leverages extensive computational resources to avoid these geometric approximations in order to accurately capture breeding behavior.

2. Methods

The ability of liquid-fueled systems to continuously remove fission products and add fissile and/or fertile elements is the main challenge for depletion simulations. The python package introduced in this work, SaltProc, takes into account online separations and feeds using the SERPENT 2 continuous-energy Monte Carlo neutron transport and depletion code. In this work, all figures of the core model were generated using the built-in SERPENT 2 plotter.

2.1. Molten Salt Breeder Reactor design and model description

The MSBR vessel has a diameter of 680 cm and a height of 610 cm. It contains a molten fluoride fuel-salt mixture that generates heat in the active core region and transports that heat to the primary heat exchanger by way of the primary salt pump. In the active core region, the fuel salt flows through channels in moderating and reflecting graphite blocks. Fuel salt at 565 °C enters the central manifold at the bottom via four 40.64-cm-diameter nozzles and flows upward through channels in the lower plenum graphite. The fuel salt exits at the top at about 704 °C through four equally spaced nozzles which connect to the salt-suction pipes leading to primary circulation pumps. The fuel salt drain lines connect to the bottom of the reactor vessel inlet manifold.

Fig. 1 shows the configuration of the MSBR vessel, including the “fission” (zone I) and “breeding” (zone II) regions inside the vessel. The core has two radial zones bounded by a solid cylindrical graphite reflector and the vessel wall. The central zone, zone I, in which 13% of the volume is fuel salt and 87% graphite, is composed of 1,320 graphite cells, 2 graphite control rods, and 2 safety⁵ rods. The under-moderated zone, zone II, with 37% fuel salt, and radial reflector, surrounds the zone I core region and serves to diminish neutron leakage. Zones I and II are surrounded radially and axially by fuel salt (**Fig. 2**). This space for fuel is necessary for injection and flow of molten salt.

Since reactor graphite experiences significant dimensional changes due to neutron irradiation, the reactor core was designed for periodic replacement. Based on the experimental irradiation data from the MSRE, the core graphite lifetime is about 4 years and the reflector graphite lifetime is 30 years (Robertson, 1971).

There are eight symmetric graphite slabs with a width of 15.24 cm in zone II, one of which is illustrated in **Fig. 2**. The holes in the centers are for the core lifting rods used during the core replacement operations. These holes also allow a portion of the fuel salt to flow to the top of the vessel for cooling the top head and axial

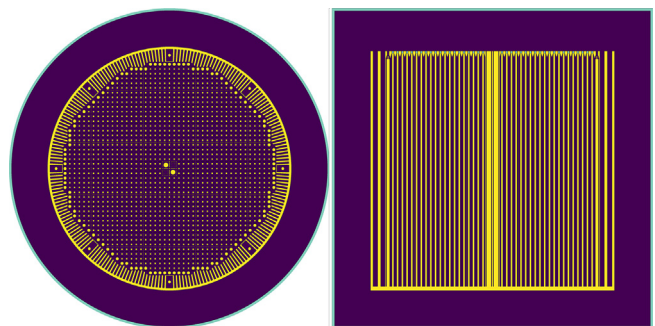


Fig. 1. Plan and elevation views of SERPENT 2 MSBR model developed in this work.

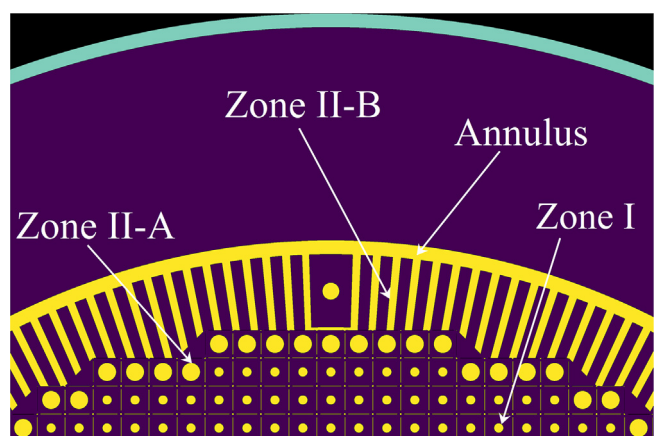


Fig. 2. Detailed view of MSBR two zone model. Yellow represents fuel salt, purple represents graphite, and aqua represents the reactor vessel. (For interpretation of the references to colour in this figure legend, the reader is referred to the web version of this article.)

reflector. **Fig. 2** also shows the 5.08-cm-wide annular space between the removable core graphite in zone II-B and the permanently mounted reflector graphite. This annulus consists entirely of fuel salt, provides space for moving the core assembly, helps compensate for the elliptical dimensions of the reactor vessel, and serves to reduce the damaging flux at the surface of the graphite reflector blocks.

^{135}Xe is a strong neutron poison, and some fraction of this gas is absorbed by graphite during MSBR operation. ORNL calculations show that for unsealed commercial graphite with helium permeability $10^{-5} \text{ cm}^2/\text{s}$ the calculated poison fraction is less than 2% (Robertson, 1971). This parameter can be improved by using experimental graphites or by applying sealing technology. The effect of the gradual poisoning of the core graphite with xenon is not treated here.

2.1.1. Core zone I

The central region of the core, called zone I, is made up of graphite elements, each $10.16 \text{ cm} \times 10.16 \text{ cm} \times 396.24 \text{ cm}$. Zone I has 4 channels for control rods: two for graphite rods which both regulate and shim during normal operation, and two for backup safety rods consisting of boron carbide clad to assure sufficient negative reactivity for emergency situations.

These graphite elements have a mostly rectangular shape with lengthwise ridges at each corner that leave space for salt flow elements. Various element sizes reduce the peak damage flux and power density in the center of the core to prevent local graphite damage. **Fig. 3** shows the elevation and plan views of graphite elements of zone I (Robertson, 1971) and their SERPENT model (Rykhlevskii et al., 2017b).

⁵ These rods needed for emergency shutdown only.

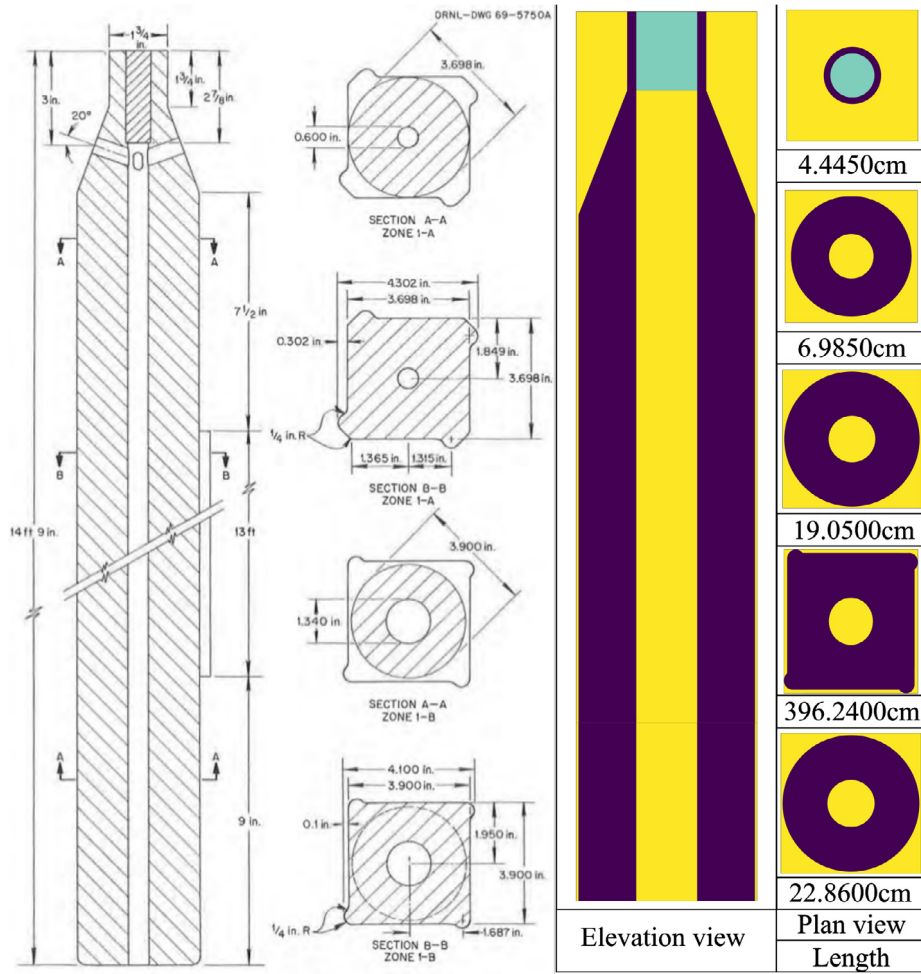


Fig. 3. Graphite moderator elements for zone I (Robertson, 1971; Rykhlevskii et al., 2017b). Yellow represents fuel salt, purple represents graphite, and aqua represents the reactor vessel. (For interpretation of the references to colour in this figure legend, the reader is referred to the web version of this article.)

2.1.2. Core zone II

Zone II, which is undermoderated, surrounds zone I. Combined with the bounding radial reflector, zone II serves to diminish neutron leakage. Two kinds of elements form this zone: large-diameter fuel channels (zone II-A) and radial graphite slats (zone II-B).

Zone II has 37% fuel salt by volume and each element has a fuel channel diameter of 6.604 cm. The graphite elements for zone II-A are prismatic with elliptical dowels running axially between the prisms. These dowels isolate the fuel salt flow in zone I from that in zone II. Fig. 4 shows the shapes and dimensions of these graphite elements and their SERPENT model. Zone II-B elements are rectangular slats spaced far enough apart to provide the 0.37 fuel salt volume fraction. The reactor zone II-B graphite 5.08 cm-thick slats vary in the radial dimension (average width is 26.67 cm) as shown in Fig. 2. Zone II serves as a blanket to achieve the best performance: a high breeding ratio and a low fissile inventory. The harder neutron energy spectrum in zone II enhances the rate of thorium resonance capture relative to the fission rate, thus limiting the neutron flux in the outer core zone and reducing the neutron leakage (Robertson, 1971).

The sophisticated, irregular shapes of the fuel elements challenge an accurate representation of zone II-B. The suggested design (Robertson, 1971) of zone II-B has 8 irregularly-shaped graphite elements as well as dozens of salt channels. These graphite elements were simplified into right-circular cylindrical shapes with central channels. Fig. 2 illustrates this core region in the SERPENT model. The volume of fuel salt in zone II was kept exactly at 37%,

so that this simplification did not considerably change the core neutronics. Simplifying the eight edge channels was the only simplification made to the MSBR geometry in this work.

2.1.3. Material composition and normalization parameters

The fuel salt, reactor graphite, and modified Hastelloy-N are all materials created at ORNL specifically for the MSBR. The initial fuel salt used the same density (3.35 g/cm^3) and composition $\text{LiF}-\text{BeF}_2-\text{ThF}_4-^{233}\text{UF}_4$ (71.75–16–12–0.25 mol%) as the MSBR design (Robertson, 1971). The lithium in the molten salt fuel is fully enriched to 100% ^7Li because ^6Li is a very strong neutron poison and becomes tritium upon neutron capture.

The JEFF-3.1.2 neutron library provided cross section generation (O.D. Bank, 2014). The specific temperature was fixed for each material and did not change during the reactor operation. The isotopic composition of each material at the initial state was described in detail in the MSBR conceptual design study (Robertson, 1971) and has been applied to the SERPENT model without any modification. Table 2 is a summary of the major MSBR parameters used by this model (Robertson, 1971).

2.2. Online reprocessing method

Removing specific chemical elements from a molten salt requires intelligent design (e.g., chemical separations equipment design, fuel salt flows to equipment) and has a considerable economic cost. All liquid-fueled MSR designs involve varying levels

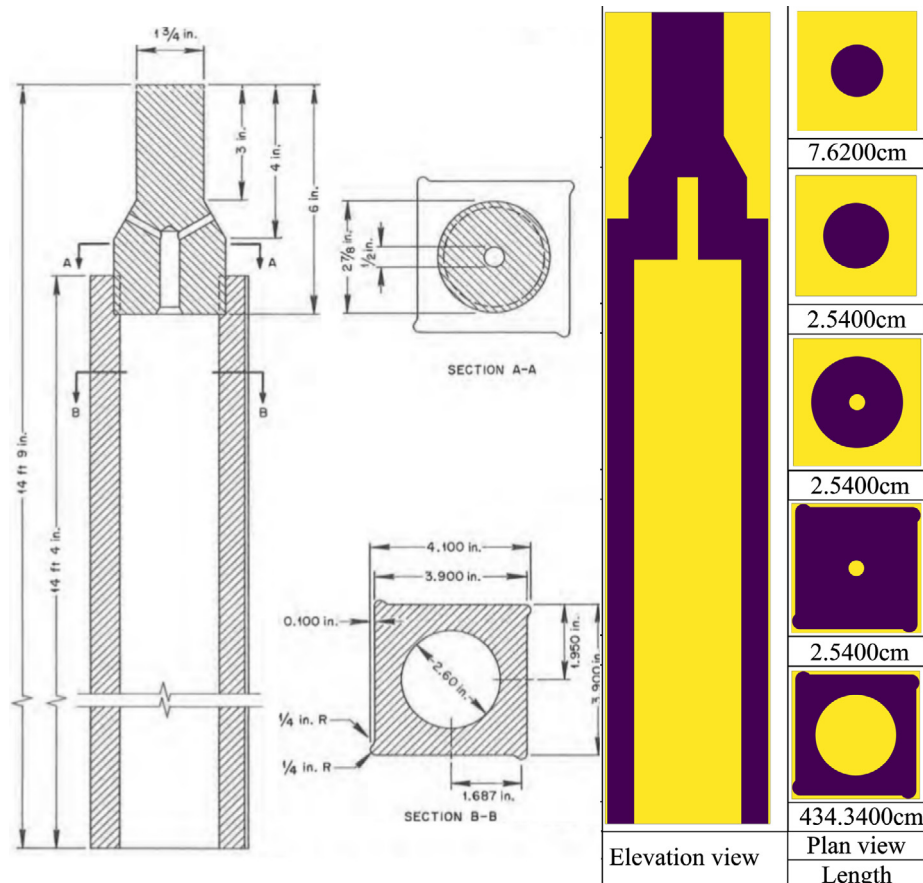


Fig. 4. Graphite moderator elements for zone II-A (Robertson, 1971; Rykhlevskii et al., 2017b). Yellow represents fuel salt and purple represents graphite. (For interpretation of the references to colour in this figure legend, the reader is referred to the web version of this article.)

Table 2
Summary of principal data for MSBR (Robertson, 1971).

Thermal capacity of reactor	2250 MW(t)
Net electrical output	1000 MW(e)
Net thermal efficiency	44.4%
Salt volume fraction in central zone I	0.13
Salt volume fraction in outer zone II	0.37
Fuel salt inventory (Zone I)	8.2 m ³
Fuel salt inventory (Zone II)	10.8 m ³
Fuel salt inventory (annulus)	3.8 m ³
Total fuel salt inventory	48.7 m ³
Fissile mass in fuel salt	1303.7 kg
Fuel salt components	LiF–BeF ₂ –ThF ₄ – ²³³ UF ₄
Fuel salt composition	71.75–16–12–0.25 mol%
Fuel salt density	3.35 g/cm ³

of online fuel processing. Minimally, volatile gaseous fission products (e.g. Kr, Xe) escape from the fuel salt during routine reactor operation and must be captured. Additional systems might be used to enhance removal of those elements. Most designs also call for the removal of noble and rare earth metals from the core since these metals act as neutron poisons. Some designs suggest a more complex list of elements to process (Fig. 5), including the temporary removal of protactinium or other regulation of the actinide inventory (Ahmad et al., 2015).

2.2.1. Fuel material flows

The ²³²Th in the fuel absorbs thermal neutrons and produces ²³³Pa which then decays into the fissile ²³³U. Furthermore, the MSBR design requires online reprocessing to remove all poisons (e.g. ¹³⁵Xe), noble metals, and gases (e.g. ⁷⁵Se, ⁸⁵Kr) every 20 s. Protac-

tinium presents a challenge, since it has a large absorption cross section in the thermal energy spectrum. Moreover, ²³³Pa left in the core would produce ²³⁴Pa and ²³⁴U, neither of which are useful as fuel. Accordingly, ²³³Pa is continuously removed from the fuel salt into a protactinium decay tank to allow ²³³Pa to decay to ²³³U without the corresponding negative neutronic impact. The reactor reprocessing system must separate ²³³Pa from the molten-salt fuel over 3 days, hold it while ²³³Pa decays into ²³³U, and return it back to the primary loop. This feature allows the reactor to avoid neutron losses to protactinium, lowers in-core fission product inventory, and increases the efficiency of ²³³U breeding. Table 3 summarizes full list of nuclides and the “cycle times”⁶ used for modeling salt treatment and separations (Robertson, 1971).

The removal rates vary among nuclides in this reactor concept which dictate the necessary resolution of depletion calculations. If the depletion time intervals are very short, an enormous number of depletion steps are required to obtain the equilibrium composition. On the other hand, if the depletion calculation time interval is too long, the impact of short-lived fission products is not captured. To compromise, a 3 day time interval was selected for depletion calculations⁷ to correlate with the removal interval of ²³³Pa and ²³²Th was continuously added to maintain the initial mass fraction of ²³²Th.

⁶ The MSBR program defined a “cycle time” as the amount of time required to remove 100% of a target nuclide from a fuel salt (Robertson, 1971).

⁷ Optimal depletion time step of 3 days for MSR batch-wise depletion simulation was first described and concluded by Powers et al. (2013).

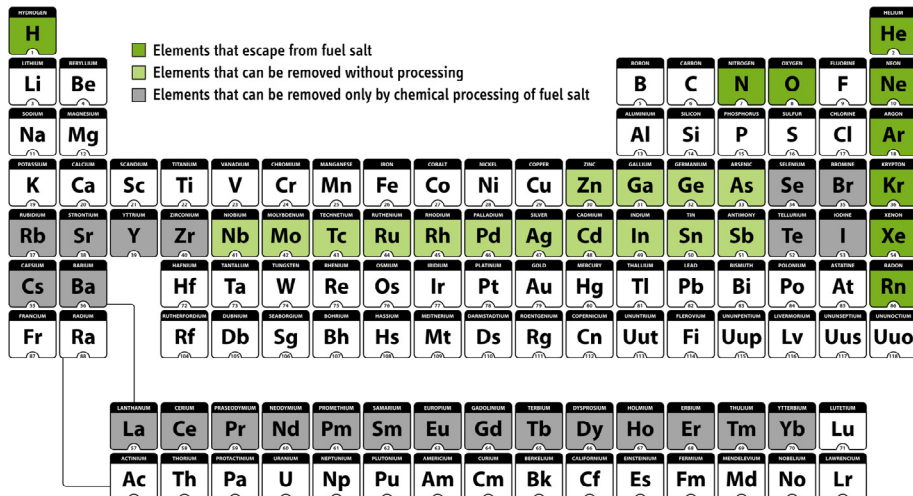


Fig. 5. Processing options for MSR fuels. Reproduced from Ahmad et al. (2015) where it was adapted from a chart courtesy of Nicolas Raymond, www.freestock.ca.

Table 3

The effective cycle times for protactinium and fission products removal (reproduced from Robertson (1971)).

Processing group	Nuclides	Cycle time (at full power)
Rare earths	Y, La, Ce, Pr, Nd, Pm, Sm, Gd	50 days
	Eu	500 days
Noble metals	Se, Nb, Mo, Tc, Ru, Rh, Pd, Ag, Sb, Te	20 s
Seminoble metals	Zr, Cd, In, Sn	200 days
Gases	Kr, Xe	20 s
Volatile fluorides	Br, I	60 days
Discard	Rb, Sr, Cs, Ba	3435 days
Protactinium	^{233}Pa	3 days
Higher nuclides	^{237}Np , ^{242}Pu	16 years

2.2.2. The SaltProc modeling and simulation code

The SaltProc tool (Rykhlevskii et al., 2018) is designed to expand SERPENT 2 depletion capabilities for modeling liquid-fueled MSR for continuous reprocessing. The Python package uses HDF5 (T.H. Group, 1997) to store data, and the PyNE Nuclear Engineering Toolkit (Scopatz et al., 2012) for SERPENT output file parsing and nuclide naming. SaltProc is an open-source tool that uses a semi-continuous approach to simulate continuous feeds and removals in MSRs.

The tool structure and capabilities of SaltProc are similar to the ChemTriton tool developed in ORNL for SCALE (Powers et al., 2013). SaltProc is coupled with the Monte Carlo SERPENT 2 software to simulate online reprocessing for irregular full-core geometry with high fidelity. The primary function of SaltProc is to manage material streams while SERPENT 2 performs the neutron transport and depletion calculations. Saltproc is defined as a python class, where each material stream is defined as a isotopic atomic density vector variable. This allows tracking of time-sensitive material streams such as the ^{233}Pa tank in the MSBR. The user can define the reprocessing parameters, such as the reprocessing interval and removal efficiency. In addition, SaltProc provides a set of functions for each stream: read and write isotopic data in/from database, separate out specific elements from stream with defined efficiency, feed in specific isotopes to stream, and maintain constant number density of specific nuclide in the core. These attributes and functions are crucial to simulating the

operation of a complex, multi-zone, multi-fluid MSR and are sufficiently general to represent myriad reactor systems.

The current version of SaltProc only allows 100% separation efficiency for either specific elements or groups of elements (e.g. Processing Groups as described in Table 3) at the end of the specific cycle time. This simplification neglects the reality that the salt spends appreciable time out of the core, in the primary loop pipes and the heat exchanger.

This approach works well for fast-removing elements (gases, noble metals, protactinium) which should be removed each depletion step. Unfortunately, for the elements with longer cycle times (i.e. rare earths should be removed every 50 days) this simplified approach leads to oscillatory behavior of all major parameters. In future releases of SaltProc, this drawback will be eliminated by removing elements with longer cycle times using different method: only mass fraction (calculated separately for each reprocessing group) will be removed each depletion step or batch (e.g. 3 days in the current work).

SaltProc, currently in active development on Github (<https://github.com/arfc/saltproc>), leverages unit tests and continuous integration for sustainable development. There is also documentation generated through Sphinx document generator for ease of use. In future releases, we plan to implement support for entirely user-customized reprocessing strategies, two-region MSR modeling capabilities, and decay modeling in tanks.

Fig. 6 illustrates the online reprocessing simulation algorithm coupling SaltProc and SERPENT 2. To perform a depletion step, SaltProc reads a user-defined SERPENT 2 template file. This file contains input cards with parameters such as geometry, material, isotopic composition, neutron population, criticality cycles, total heating power, and boundary conditions. After the depletion calculation, SaltProc reads the depleted fuel composition file and stores the depleted composition isotopic vector in an HDF5 database.

SaltProc only stores and edits the isotopic composition of the fuel stream, which makes SaltProc a flexible tool to model any geometry: an infinite medium, a unit cell, a multi-zone simplified assembly, or a full core. This flexibility allows the user to perform simulations of varying fidelity and computational intensity.

SaltProc can manage as many material streams as desired. It also may work with multiple depletion materials. At the end of each depletion step, SaltProc reads the depleted compositions and tracks each material stream individually. Following this, it applies chemical separation functions to fuel stream vectors. These vectors then form a matrix (isotopics \times timesteps) which SaltProc

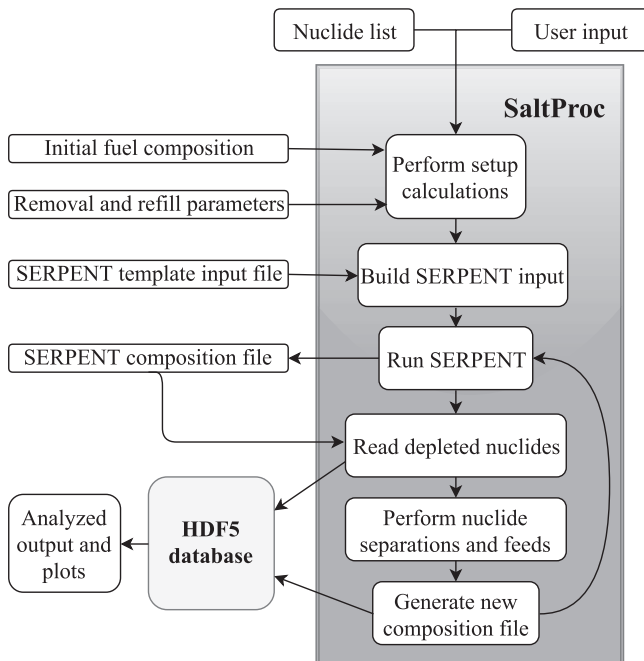


Fig. 6. Flow chart for the Saltproc python package.

stores in an HDF5 database and prints into the SERPENT 2 composition file for the next depletion calculation.

SaltProc records every value every timestep. The resulting time series datasets produced by SaltProc are listed below, where the values inside the parenthesis are the dataset sizes:

- core adensity before reproc (number of isotopes × timesteps)
- core adensity after reproc (number of isotopes × timesteps)
- Keff_BOE (1 × timesteps)
- Keff_EOE (1 × timesteps)
- Th tank adensity (number of isotopes × timesteps)
- iso codes (number of isotopes × 1)

In addition, SaltProc is able to define time-dependent material feed and removal rates to investigate their impacts. These rates need not be constant in SaltProc. They can be defined as piecewise functions or set to respond to conditions in the core. For instance, SaltProc might increase the fissile material feeding rate if the effective multiplication factor, k_{eff} , falls below a specific limit (e.g., 1.002). These capabilities allow SaltProc to analyze fuel cycle of a generic liquid-fueled MSR. In summary, the development approach of SaltProc focused on producing a generic, flexible and expandable tool to give the SERPENT 2 Monte Carlo code the ability to conduct advanced in-reactor fuel cycle analysis as well as simulate a myriad of online refueling and fuel reprocessing systems.

3. Results

The SaltProc online reprocessing simulation package is demonstrated in four applications: (1) analyzing MSBR neutronics and fuel cycle to find the equilibrium core composition and core depletion, (2) studying operational and safety parameters evolution during MSBR operation, (3) demonstrating that in a single-fluid two-region MSBR conceptual design the undermoderated outer core zone II works as a virtual “blanket”, reduces neutron leakage and improves breeding ratio due to neutron energy spectral shift, and

- (4) determining the effect of fission product removal on the core neutronics.

The neutron population per cycle and the number of active/inactive cycles were chosen to obtain balance between reasonable uncertainty for a transport problem ($\leq 15 \text{ pcm}$ ⁸ for effective multiplication factor) and computational time. The MSBR depletion and safety parameter computations were performed on 64 Blue Waters XK7 nodes (two AMD 6276 Interlagos CPU per node, 16 floating-point Bulldozer core units per node or 32 “integer” cores per node, nominal clock speed is 2.45 GHz). The total computational time for calculating the equilibrium composition was approximately 9,900 node-hours (18 core-years.).

3.1. Effective multiplication factor

Figs. 7, 8 show the effective multiplication factors obtained using SaltProc and SERPENT2. The effective multiplication factors were calculated after removing fission products listed in Table 3 and adding the fertile material at the end of cycle time (3 days for this work). The effective multiplication factor fluctuates significantly as a result of the batch-wise nature of this online reprocessing strategy.

First, SERPENT calculates the effective multiplication factor for the beginning of the cycle (there is fresh fuel composition at the first step). Next, it computes the new fuel salt composition at the end of a 3-day depletion. The corresponding effective multiplication factor is much smaller than the previous one. Finally, SERPENT calculates k_{eff} for the depleted composition after applying feeds and removals. The K_{eff} increases accordingly since major reactor poisons (e.g. Xe, Kr) are removed, while fresh fissile material (^{233}U) from the protactinium decay tank is added.

Additionally, the presence of rubidium, strontium, cesium, and barium in the core are disadvantageous to reactor physics. Overall, the effective multiplication factor gradually decreases from 1.075 to ≈ 1.02 at equilibrium after approximately 6 years of irradiation.

In fact, SaltProc fully removes all of these elements every 3435 days (not a small mass fraction every 3 days) which causes the multiplication factor to jump by approximately 450 pcm, and limits using the batch approach for online reprocessing simulations. In future versions of SaltProc this drawback will be eliminated by removing elements with longer residence times (seminoble metals, volatile fluorides, Rb, Sr, Cs, Ba, Eu). In that approach, chemistry models will inform separation efficiencies for each reprocessing group and removal will optionally be spread more evenly across the cycle time.

3.2. Fuel salt composition dynamics

The analysis of the fuel salt composition evolution provides more comprehensive information about the equilibrium state. Fig. 9 shows the number densities of major nuclides which have a strong influence on the reactor core physics. The concentration of ^{233}U , ^{232}Th , ^{233}Pa , and ^{232}Pa in the fuel salt change insignificantly after approximately 2500 days of operation. In particular, the ^{233}U number density fluctuates by less than 0.8% between 16 and 20 years of operation. Hence, a quasi-equilibrium state was achieved after 16 years of reactor operation. In contrast, a wide variety of nuclides, including fissile isotopes (e.g. ^{235}U) and non-fissile strong absorbers (e.g. ^{234}U), kept accumulating in the core. Fig. 10 demonstrates production of fissile isotopes in the core. In the end of the considered operational time, the core contained significant ^{235}U ($\approx 10^{-5} \text{ atom/b-cm}$), ^{239}Pu ($\approx 5 \times 10^{-7} \text{ atom/b-cm}$), and ^{241}Pu

⁸ 1 pcm = $10^{-5} \Delta k_{\text{eff}} / k_{\text{eff}}$.

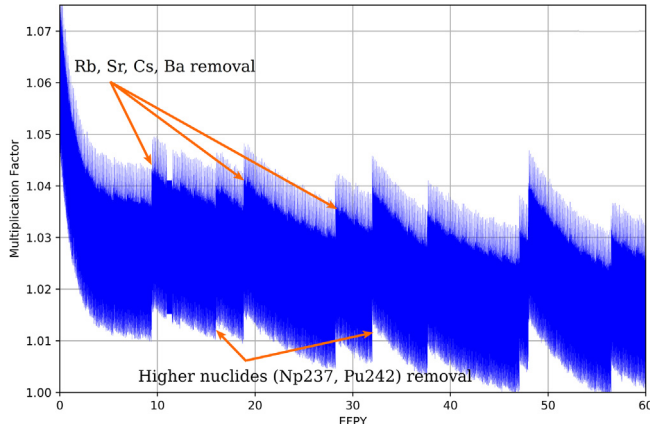


Fig. 7. Effective multiplication factor dynamics for full-core MSBR model over a 60-year reactor operation lifetime.

($\approx 5 \times 10^{-7}$ atom/b-cm). Meanwhile, the equilibrium number density of the target fissile isotope ^{233}U was approximately 7.97×10^{-5} atom/b-cm. Small dips in neptunium and plutonium number density every 16 years are caused by removing ^{237}Np and ^{242}Pu (included in Processing group "Higher nuclides", see Table 3) which decay into ^{235}Np and ^{239}Pu , respectively. Thus, production of new fissile materials in the core, as well as ^{233}U breeding, made it possible to compensate for negative effects of strong absorber accumulation and keep the reactor critical.

3.3. Neutron spectrum

Fig. 11 shows the normalized neutron flux spectrum for the full-core MSBR model in the energy range from 10^{-8} to 10 MeV. The neutron energy spectrum at equilibrium is harder than at startup due to plutonium and other strong absorbers accumulating in the core during reactor operation.

Fig. 12 shows that zone I produced more thermal neutrons than zone II, corresponding to a majority of fissions occurring in the central part of the core. In the undermoderated zone II, the neutron energy spectrum is harder, which leads to more neutrons capture

by ^{232}Th and helps achieve relatively high breeding ratio. Moreover, the (n,γ) resonance energy range in ^{232}Th is from 10^{-4} to 10^{-2} MeV. Therefore, the moderator-to-fuel ratio for zone II was chosen to shift the neutron energy spectrum in this range. Furthermore, in the central core region (zone I), the neutron energy spectrum shifts to a harder spectrum over 20 years of reactor operation. Meanwhile, in the outer core region (zone II), a similar spectral shift takes place at a reduced scale. These results are in a good agreement with original ORNL report (Robertson, 1971) and the most recent whole-core steady-state study (Park et al., 2015).

It is important to obtain the epithermal and thermal spectra to produce ^{233}U from ^{232}Th because the radiative capture cross section of thorium decreases monotonically from 10^{-10} MeV to 10^{-5} MeV. Hardening the spectrum tends to significantly increase resonance absorption in thorium and decrease absorptions in fissile and construction materials.

3.4. Neutron flux

Fig. 13 shows the radial distribution of fast and thermal neutron flux for the both initial and equilibrium composition. The neutron fluxes have similar shapes for both compositions but the equilibrium case has a harder spectrum. A significant spectral shift was observed in the central region of the core (zone I), while for the outer region (zone II), it is negligible for fast but notable for thermal neutrons. These neutron flux radial distributions agree with the fluxes in the original ORNL report (Robertson, 1971). Overall, spectrum hardening during MSBR operation should be carefully studied when designing the reactivity control system.

3.5. Power and breeding distribution

Table 4 shows the power fraction in each zone for initial and equilibrium fuel compositions. Fig. 14 reflects the normalized power distribution of the MSBR quarter core for equilibrium fuel salt composition. For both the initial and equilibrium compositions, fission primarily occurs in the center of the core, namely zone I. The spectral shift during reactor operation results in slightly different power fractions at startup and equilibrium, but most of the power is still generated in zone I at equilibrium (Table 4). Fig. 15 shows the neutron capture reaction rate distribution for

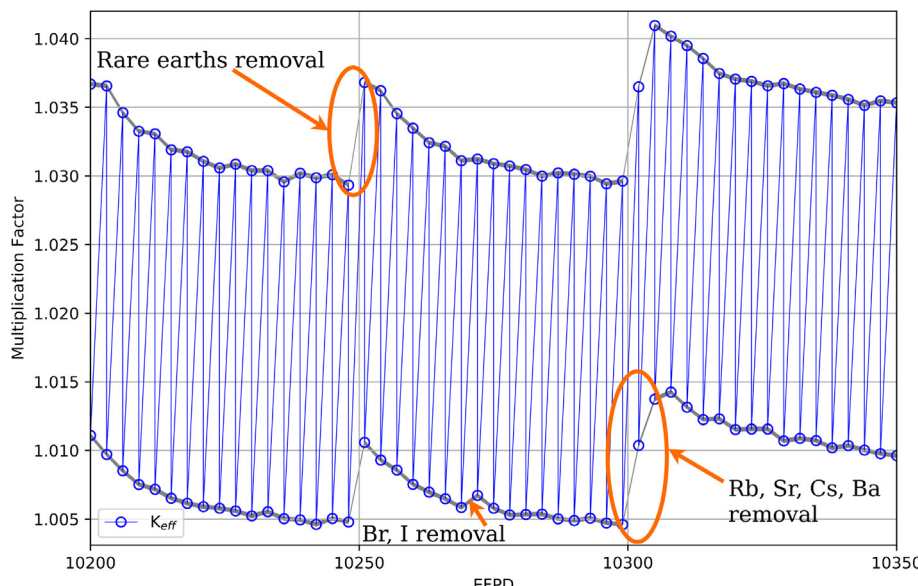


Fig. 8. Zoomed effective multiplication factor for 150-EFPD time interval.

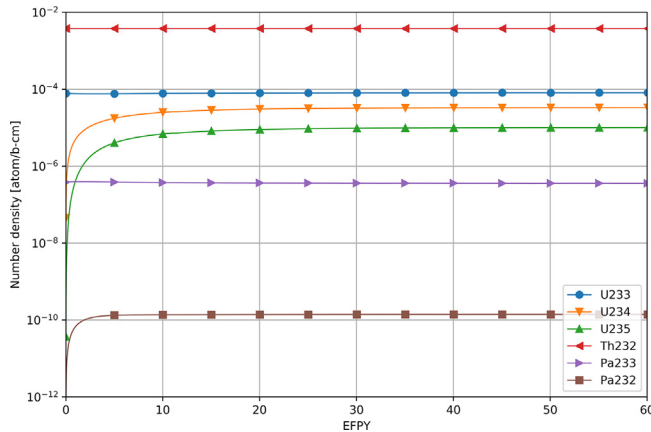


Fig. 9. Number density of major nuclides during 60 years of reactor operation.

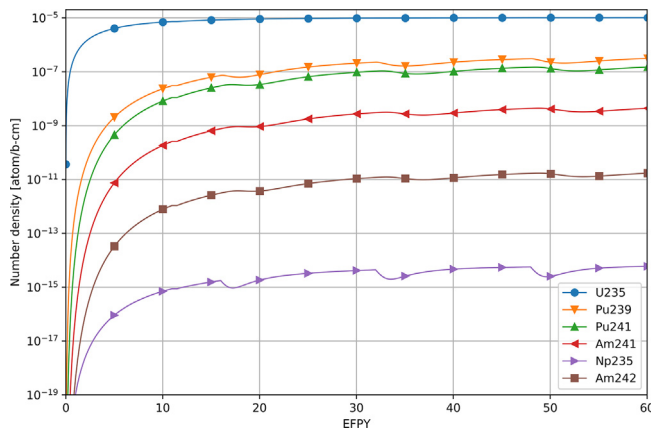


Fig. 10. Number density of fissile in epithermal spectrum nuclides accumulation during the reactor operation.

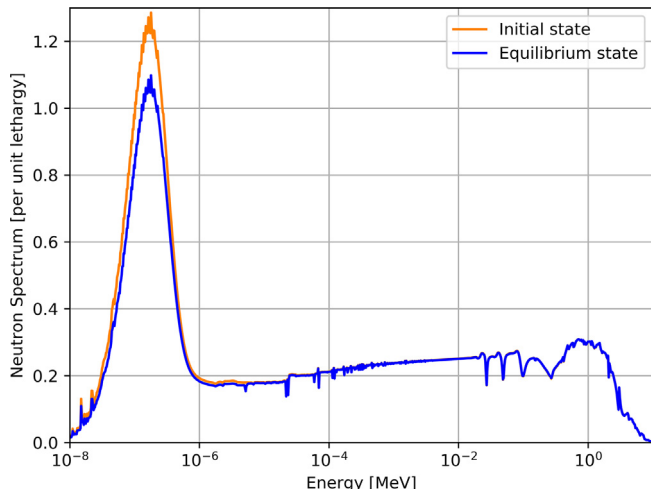


Fig. 11. The neutron flux energy spectrum is normalized by unit lethargy and the area under the curve is normalized to 1 for initial and equilibrium fuel salt composition.

^{232}Th normalized by the total neutron flux for initial and equilibrium states. The distribution reflects the spatial distribution of ^{233}U production in the core. ^{232}Th neutron capture produces ^{233}Th which then β -decays to ^{233}Pa , the precursor for ^{233}U production. Accordingly, this characteristic represents the breeding

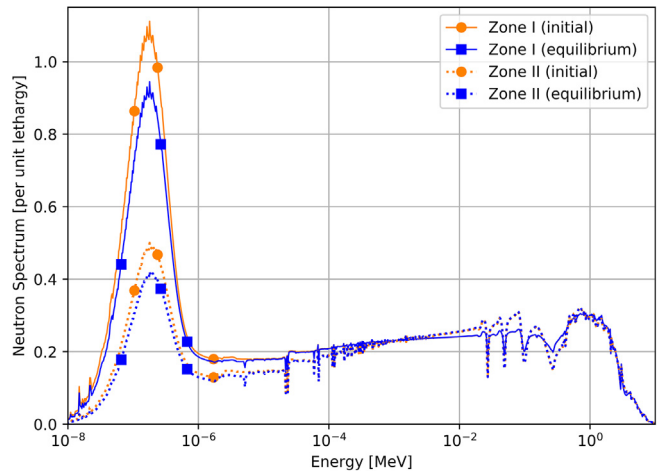


Fig. 12. The neutron flux energy spectrum in different core regions is normalized by unit lethargy and the area under the curve is normalized to 1 for the initial and equilibrium fuel salt composition.

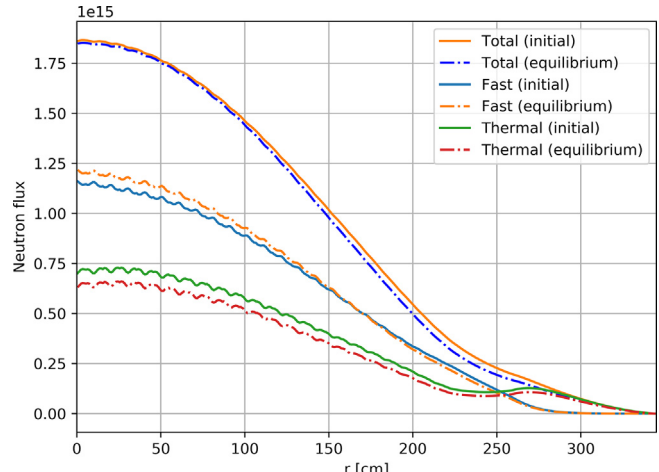


Fig. 13. Radial neutron flux distribution for initial and equilibrium fuel salt composition.

Table 4

Power generation fraction in each zone for initial and equilibrium state.

Core region	Initial	Equilibrium
Zone I	97.91%	98.12%
Zone II	2.09%	1.88%

distribution in the MSBR core. Spectral shift does not cause significant changes in power nor in breeding distribution. Even after 20 years of operation, most of the power is still generated in zone I.

3.6. Temperature coefficient of reactivity

Table 5 summarizes temperature effects on reactivity calculated in this work for both initial and equilibrium fuel compositions, compared with the original ORNL report data (Robertson, 1971). By propagating the k_{eff} statistical error provided by SERPENT2, uncertainty for each temperature coefficient was obtained and appears in **Table 5**. Other sources of uncertainty are neglected, such as cross section measurement error and approximations inherent in the equations of state providing both the salt and graphite

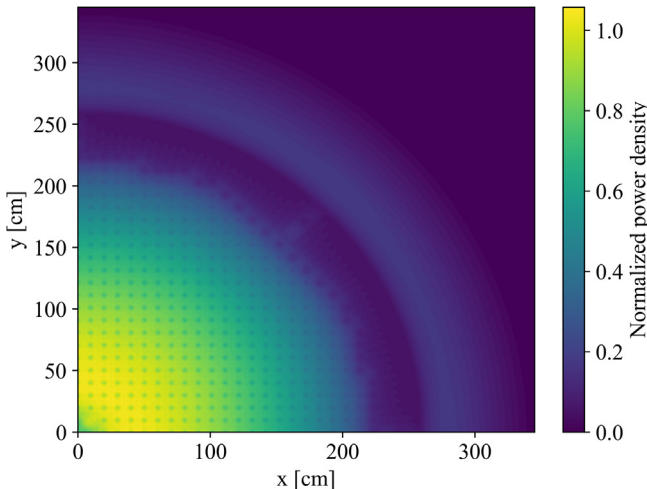


Fig. 14. Normalized power density for equilibrium fuel salt composition.

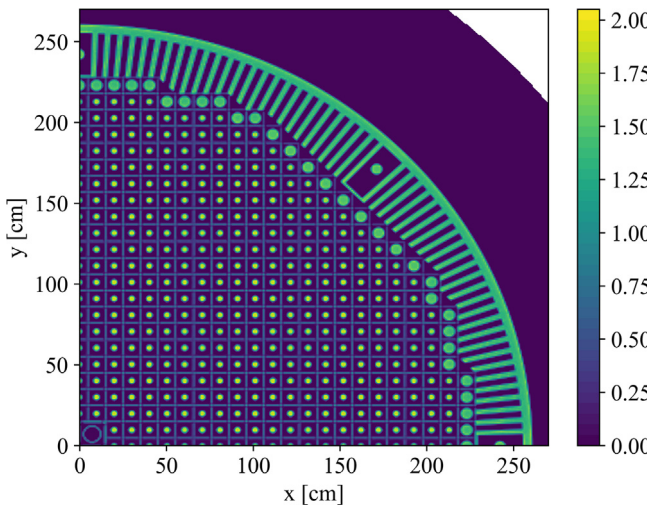


Fig. 15. ^{232}Th neutron capture reaction rate normalized by total flux for equilibrium fuel salt composition.

density dependence on temperature. The main physical principle underlying the reactor temperature feedback is an expansion of heated material. When the fuel salt temperature increases, the density of the salt decreases, but at the same time, the total volume of fuel salt in the core remains constant because it is bounded by the graphite. When the graphite temperature increases, the density of graphite decreases, creating additional space for fuel salt. To determine the temperature coefficients, the cross section temperatures for the fuel and moderator were changed from 900 K to 1000 K. Three different cases were considered:

1. Temperature of fuel salt rising from 900 K to 1000 K.
2. Temperature of graphite rising from 900 K to 1000 K.
3. Whole reactor temperature rising from 900 K to 1000 K.

In the first case, changes in the fuel temperature only impact fuel density. In this case, the geometry is unchanged because the fuel is a liquid. However, when the moderator heats up, both the density and the geometry change due to thermal expansion of the solid graphite blocks and reflector. Accordingly, the new graphite density was calculated using a linear temperature expansion coefficient of $1.3 \times 10^{-6} \text{K}^{-1}$ (Robertson, 1971). A new geometry input for SERPENT2, which takes into account displacement of

Table 5
Temperature coefficients of reactivity for initial and equilibrium state.

Reactivity coefficient	Initial [pcm/k]	Equilibrium [pcm/k]	Reference (Initial) (Robertson, 1971)
Doppler in fuel salt	-4.73 ± 0.038	-4.69 ± 0.038	-4.37
Fuel salt density	$+1.21 \pm 0.038$	$+1.66 \pm 0.038$	+1.09
Total fuel salt	-3.42 ± 0.038	-2.91 ± 0.038	-3.22
Graphite spectral shift	$+1.56 \pm 0.038$	$+1.27 \pm 0.038$	
Graphite density	$+0.14 \pm 0.038$	$+0.23 \pm 0.038$	
Total moderator (graphite)	$+1.69 \pm 0.038$	$+1.35 \pm 0.038$	+2.35
Total core	-1.64 ± 0.038	-1.58 ± 0.038	-0.87

graphite surfaces, was created based on this information. For calculation of displacement, it was assumed that the interface between the graphite reflector and vessel did not move, and that the vessel temperature did not change. This is the most reasonable assumption for the short-term reactivity effects because inlet salt is cooling graphite reflector and inner surface of the vessel.

The fuel temperature coefficient (FTC) is negative for both initial and equilibrium fuel compositions due to thermal Doppler broadening of the resonance capture cross sections in the thorium. A small positive effect of fuel density on reactivity increases from $+1.21 \text{ pcm/K}$ at reactor startup to $+1.66 \text{ pcm/K}$ for equilibrium fuel composition which has a negative effect on FTC magnitude during the reactor operation. This is in good agreement with earlier research (Robertson, 1971; Park et al., 2015). The moderator temperature coefficient (MTC) is positive for the startup composition and decreases during reactor operation because of spectrum hardening with fuel depletion. Finally, the total temperature coefficient of reactivity is negative for both cases, but decreases during reactor operation due to spectral shift. In summary, even after 20 years of operation the total temperature coefficient of reactivity is relatively large and negative during reactor operation (comparing with conventional PWR which has temperature coefficient about -3.08 pcm/K (Forget et al., 2018)), despite positive MTC, and affords excellent reactor stability and control.

3.7. Reactivity control system rod worth

Table 6 summarizes the reactivity control system worth. During normal operation, the control (graphite) rods are fully inserted, and the safety (B_4C) rods are fully withdrawn. To insert negative reactivity into the core, the graphite rods are gradually withdrawn from the core. In an accident, the safety rods would be dropped down into the core. The integral rod worths were calculated for various positions to separately estimate the worth of the control graphite rods⁹, the safety (B_4C) rods, and the whole reactivity control system. Control rod integral worth is approximately 28 cents and stays almost constant during reactor operation. The safety rod integral worth decreases by 16.2% during 20 years of operation because of neutron spectrum hardening and absorber accumulation in proximity to reactivity control system rods. This 16% decline in control system worth should be taken into account in MSBR accident analysis and safety justification.

3.8. Six factor analysis

The effective multiplication factor can be expressed using the following formula:

⁹ In Robertson (1971), the graphite rods are referred to as "control" rods.

Table 6

Control system rod worth for initial and equilibrium fuel composition.

Reactivity parameter [cents]	Initial	Equilibrium
Control (graphite) rod integral worth	28.2 ± 0.8	29.0 ± 0.8
Safety (B_4C) rod integral worth	251.8 ± 0.8	211.0 ± 0.8
Total reactivity control system worth	505.8 ± 0.7	424.9 ± 0.8

$$k_{\text{eff}} = k_{\text{inf}} P_f P_t = \eta \epsilon p f P_f P_t$$

[Table 7](#) summarizes the six factors for both initial and equilibrium fuel salt composition. Using SERPENT2 and SaltProc, these factors and their statistical uncertainties have been calculated for both initial and equilibrium fuel salt composition (see [Table 2](#)). The fast and thermal non-leakage probabilities remain constant despite the evolving neutron spectrum during operation. In contrast, the neutron reproduction factor (η), resonance escape probability (p), and fast fission factor (ϵ) are considerably different between startup and equilibrium. As indicated in [Fig. 11](#), the neutron spectrum is softer at the beginning of reactor life. Neutron spectrum hardening causes the fast fission factor to increase through the core lifetime. The opposite is true for the resonance escape probability. Finally, the neutron reproduction factor decreases during reactor operation due to accumulation of fissile plutonium isotopes.

3.9. Thorium refill rate

In a MSBR reprocessing scheme, the only external feed material flow is ^{232}Th . [Fig. 16](#) shows the ^{232}Th feed rate calculated for 60 years of reactor operation. The ^{232}Th feed rate fluctuates significantly as a result of the batch-wise nature of this online reprocessing approach. [Fig. 17](#) shows zoomed thorium feed rate for short 150-EFPD interval. Note that the large spikes of up to 36 kg/day in a thorium consumption occurs every 3435 days. This is required due to strong absorbers (Rb, Sr, Cs, Ba) removal at the end of effective cycle (100% of these elements removing every 3435 days of operation). The corresponding effective multiplication factor increase ([Fig. 7](#)) and breeding intensification leads to additional ^{232}Th consumption.

The average thorium feed rate increases during the first 500 days of operation, and steadily decreases due to spectrum hardening and accumulation of absorbers in the core. As a result, the average ^{232}Th feed rate over 60 years of operation is about 2.40 kg/day. This thorium consumption rate is in good agreement with a recent online reprocessing study by ORNL ([Betzler et al., 2017a](#)). At equilibrium, the thorium feed rate is determined by the reactor power, the energy released per fission, and the neutron energy spectrum.

3.10. The effect of removing fission product from fuel salt

Loading initial fuel salt composition into the MSBR core leads to a supercritical configuration ([Fig. 18](#)). After reactor startup, the effective multiplication factor for the case with volatile gases and noble metals removal is approximately 7500 pcm higher than for case with no fission products removal. This significant impact on the reactor core is achieved due to immediate removal (20 s cycle time) and high absorption cross section of Xe, Kr, Mo, and other noble metals removed. The effect of rare earth element removal is considerable a few months after startup and reached approximately 5500 pcm after 10 years of operation. The rare earth elements were removed at a slower rate (50-day cycle time). Moreover, [Fig. 18](#) demonstrates that batch-wise removal of strong absorbers every 3 days did not necessarily leads to fluctuation in results but rare earth elements removal every 50 days causes an approximately 600 pcm jump in reactivity.

Table 7

Six factors for the full-core MSBR model for initial and equilibrium fuel composition.

Factor	Initial	Equilibrium
Neutron reproduction factor (η)	$1.3960 \pm .000052$	$1.3778 \pm .00005$
Thermal utilization factor (f)	$0.9670 \pm .000011$	$0.9706 \pm .00004$
Resonance escape probability (p)	$0.6044 \pm .000039$	$0.5761 \pm .00004$
Fast fission factor (ϵ)	$1.3421 \pm .000040$	$1.3609 \pm .00004$
Fast non-leakage probability (P_f)	$0.9999 \pm .000004$	$0.9999 \pm .000004$
Thermal non-leakage probability (P_t)	$0.9894 \pm .000005$	$0.9912 \pm .00005$

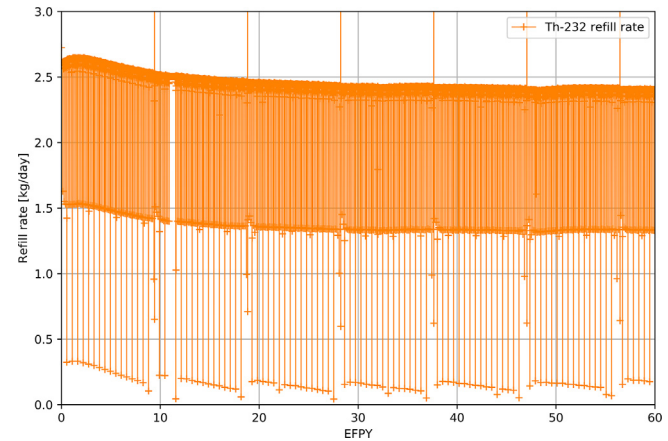


[Fig. 16.](#) ^{232}Th feed rate over 60 years of MSBR operation.

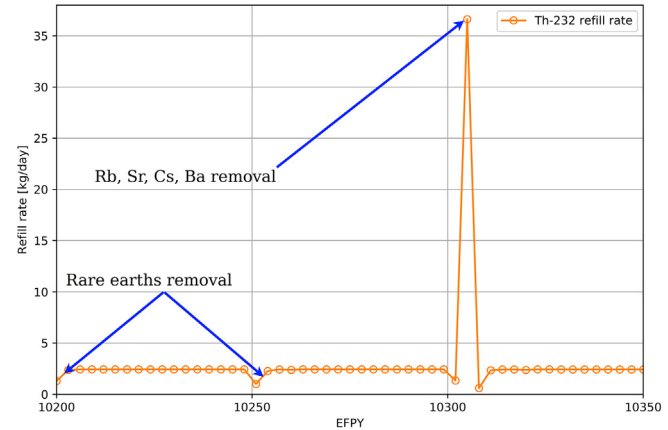


[Fig. 17.](#) Zoomed ^{232}Th feed rate for 150-EFPD time interval.

The effective multiplication factor of the core reduces gradually over operation time because the fissile material (^{233}U) continuously depletes from the fuel salt due to fission while fission products accumulate in the fuel salt simultaneously. Eventually, without fission products removal, the reactivity decreases to the subcritical state after approximately 500 and 1300 days of operation for cases with no removal and volatile gases & noble metals removal, respectively. The time when the simulated core reaches subcriticality ($k_{\text{eff}} < 1.0$) for full-core model) is called the core lifetime. Therefore, removing fission products provides with significant neutronic benefit and enables a longer core lifetime.

4. Discussion and conclusions

This work introduces the open source MSR simulation package SaltProc. SaltProc expands the capability of SERPENT2, the continuous-energy Monte Carlo code to include online reprocess-

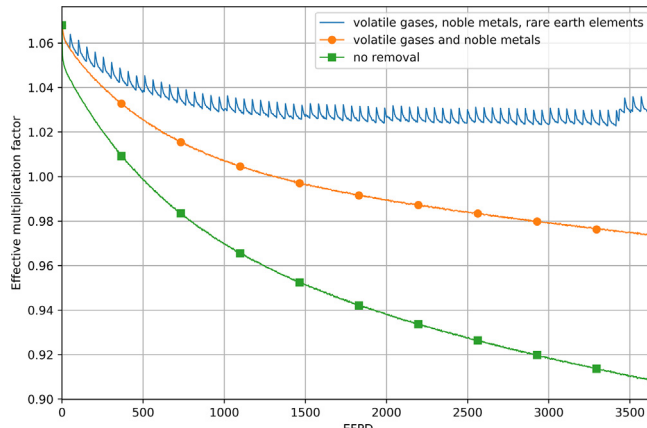


Fig. 18. Calculated effective multiplication factor for full-core MSBR model with removal of various fission product groups over 10 years of operation.

ing modeling capabilities (Rykhlevskii et al., 2018). Benefits of SaltProc include generic geometry modeling, multi-flow capabilities, time-dependent feed and removal rates, and the ability to specify removal efficiency. The main goal of this work has been to demonstrate SaltProc's capability to find the equilibrium fuel salt composition (where equilibrium is defined as when the number densities of major isotopes vary by less than 1% over several years). A secondary goal has been to compare predicted operational and safety parameters (e.g., neutron energy spectrum, power and breeding distribution, temperature coefficients of reactivity) of the MSBR at startup and equilibrium state. A tertiary goal has been to demonstrate benefits of continuous fission products removal for thermal MSR design.

To achieve these goals, a full-core high-fidelity benchmark model of the MSBR was implemented in SERPENT2. The full-core model was used instead of the simplified single-cell model (Betzler et al., 2017a; Rykhlevskii et al., 2017a; Betzler et al., 2018) to precisely describe the two-region MSBR concept design sufficiently to accurately represent breeding in the outer core zone. When running depletion calculations, the most important fission products and ^{233}Pa are removed while fertile and fissile materials are added to the fuel salt every 3 days. Meanwhile, the removal interval for the rare earths, volatile fluorides, and seminoble metals was greater than month a (50 days), which caused effective multiplication factor fluctuation.

4.1. Equilibrium state search

The results of this study indicate that the effective multiplication factor slowly decreases from 1.075 and reaches 1.02 at equilibrium after approximately 6 years of operation. At the same time, the concentrations of ^{233}U , ^{232}Th , ^{233}Pa , ^{232}Pa stabilized after approximately 2500 days of operation. Particularly, ^{233}U number density equilibrates¹⁰ after 16 years of operation. Consequently, the core reaches the quasi-equilibrium state after 16 years of operation. However, a wide variety of nuclides, including fissile isotopes (e.g. ^{233}U , ^{239}Pu) and non-fissile strong absorbers (e.g. ^{234}U), continue accumulating in the core.

4.2. Spectral shift

We also found that the neutron energy spectrum grew harder as the core approaches equilibrium because significant heavy fission

products accumulated in the MSBR core. Moreover, the neutron energy spectrum in the central core region is much softer than in the outer core region due to lower moderator-to-fuel ratio in the outer zone, and this distribution remains stable during reactor operation. Finally, the epithermal or thermal spectrum is needed to effectively breed ^{233}U from ^{232}Th because radiative capture cross section of thorium-232 monotonically decreases from 10^{-10} MeV to 10^{-5} MeV. A harder spectrum in the outer core region tends to significantly increase resonance absorption in thorium and decrease the absorptions in fissile and structural materials.

The spatial power distribution in the MSBR shows that 98% of the fission power is generated in central zone I, and neutron energy spectral shift did not cause any notable changes in a power distribution. The spatial distribution of neutron capture reaction rate for fertile ^{232}Th , corresponding to breeding in the core, confirms that most of the breeding occurs in an outer, undermoderated, region of the MSBR core. Finally, the average ^{232}Th refill rate throughout 60 years of operation is approximately 2.40 kg/day or 100 g/GWh_e.

We compared the safety parameters for the initial fuel loading and equilibrium compositions using the SERPENT2 Monte Carlo code. The total temperature coefficient is large and negative at startup and equilibrium but the magnitude decreases throughout reactor operation from -3.10 to -0.94 pcm/K as the spectrum hardens. The moderator temperature coefficient is positive and also decreases during fuel depletion. The reactivity control system efficiency analysis showed that the safety rod integral worth decreases by approximately 16.2% over 16 years of operation, while graphite rod integral worth remains constant. Therefore, neutron energy spectrum hardening during fuel salt depletion has an undesirable impact on MSBR stability and controllability, and should be taken into consideration in further analysis of transient accident scenarios.

4.3. Benefits of fission product removal

The MSBR core performance benefits from the removal of volatile gases, noble metals, and rare earths from the fuel salt. Moreover, immediate removal of volatile gases (e.g., xenon) and noble metals increased reactivity by approximately 7500 pcm over a 10-year timeframe. In contrast, the effect of relatively slower removal of rare earth elements (every 50 days cycle instead of 3 days) has less impact (5500 pcm) on the core reactivity after 10 years of operation. An additional study is needed to establish neutronic and economic tradeoffs of removing each element.

4.4. Future work

SaltProc-SERPENT coupled simulation efforts could progress in a number of different directions. First optimization of reprocessing parameters (e.g. time step, feeding rate, protactinium removal rate) could establish the best fuel utilization, breeding ratio, or safety characteristics for various designs. This might be performed with a parameter sweeping outer loop which would change an input parameter by a small increment, run the simulation and analyze output to determine optimal configuration. Alternatively, the existing RAVEN optimization framework (Alfonsi et al., 2013) might be employed for such optimization studies.

Only the batch-wise online reprocessing approach has been treated in this work. However, the SERPENT2 Monte Carlo code was extended for continuous online fuel reprocessing simulation (Aufiero et al., 2013). This extension must be verified against existing SaltProc/SERPENT or ChemTriton/SCALE packages, and could be employed for immediate removal of fission product gases (e.g., Xe, Kr) which have a strong negative impact on core lifetime and breeding efficiency. Finally, using the built-in SERPENT2 Monte

¹⁰ fluctuates less than 0.8%.

Carlo code online reprocessing & refueling material burnup routine would significantly speed up computer-intensive full-core depletion simulations.

Acknowledgments

This research is part of the Blue Waters sustained-petascale computing project, which is supported by the National Science Foundation (awards OCI-0725070 and ACI-1238993) and the state of Illinois. Blue Waters is a joint effort of the University of Illinois at Urbana-Champaign and its National Center for Supercomputing Applications

The authors would like to thank members of the Advanced Reactors and Fuel Cycles (ARFC) group at the University of Illinois – Urbana Champaign who provided valuable code reviews and proofreading.

The authors contributed to this work as described below. Andrei Rykhlevskii conceived and designed the simulations, wrote the paper, prepared figures and/or tables, performed the computation work, contributed to the software product, and reviewed drafts of the paper. Jin Whan Bae conceived and designed the simulations, wrote the paper, contributed to the software product, and reviewed drafts of the paper. Andrei Rykhlevskii is supported by DOE ARPA-E MEITNER program award 1798-1576. Jin Whan Bae is supported by funding received from the DOE Nuclear Energy University Program (Project 16-10512) 'Demand-Driven Cycamore Archetypes'.

Kathryn D. Huff directed and supervised the work, conceived and designed the simulations, contributed to the software product, and reviewed drafts of the paper. Prof. Huff is supported by the Nuclear Regulatory Commission Faculty Development Program, the National Center for Supercomputing Applications, the NNSA Office of Defense Nuclear Nonproliferation R&D through the Consortium for Verification Technologies and the Consortium for Non-proliferation Enabling Capabilities, the International Institute for Carbon Neutral Energy Research (WPI-I2CNER), sponsored by the Japanese Ministry of Education, Culture, Sports, Science and Technology, and DOE ARPA-E MEITNER program award 1798-1576.

References

- Ahmad, A., McClamrock, E.B., Glaser, A., 2015. Neutronics calculations for denatured molten salt reactors: assessing resource requirements and proliferation-risk attributes. *Ann. Nucl. Energy* 75, 261–267. <https://doi.org/10.1016/j.anucene.2014.08.014>. URL<http://www.sciencedirect.com/science/article/pii/S0306454914003995>.
- Alfonsi, A., Rabiti, C., Mandelli, D., Cogliati, J., Kinoshita, R., 2013. Raven as a tool for dynamic probabilistic risk assessment: software overview. In: Proceeding of M&C2013 International Topical Meeting on Mathematics and Computation.
- Ashraf, O., Smirnov, A.D., Tikhomirov, G.V., 2018. Nuclear fuel optimization for molten salt fast reactor. In: Journal of Physics: Conference Series, vol. 1133. IOP Publishing, p. 012026.
- Aufiero, M., Cammi, A., Fiorina, C., Leppänen, J., Luzzi, L., Ricotti, M.E., 2013. An extended version of the SERPENT-2 code to investigate fuel burn-up and core material evolution of the Molten Salt Fast Reactor. *J. Nucl. Mater.* 441 (1–3), 473–486. <https://doi.org/10.1016/j.jnucmat.2013.06.026>. URL<http://www.sciencedirect.com/science/article/pii/S0022311513008507>.
- Bauman, H.F., Cunningham III, G.W., Lucius, J.L., Kerr, H.T., Craven, C.W.J., 1971. Rod A Nuclear and Fuel-Cycle Analysis Code for Circulating-Fuel Reactors. Oak Ridge National Lab., Tenn. <https://doi.org/10.2172/4741221>. Tech. Rep. ORNL-TM-3359.
- Betzler, B.R., Powers, J.J., Worrall, A., 2016. Modeling and simulation of the start-up of a thorium-based molten salt reactor. *Proc. Int. Conf. Physor*.
- Betzler, B.R., Powers, J.J., Worrall, A., 2017a. Molten salt reactor neutronics and fuel cycle modeling and simulation with SCALE. *Ann. Nucl. Energy* 101 (Supplement C), 489–503. <https://doi.org/10.1016/j.anucene.2016.11.040>. URL<http://linkinghub.elsevier.com/retrieve/pii/S0306454916309185>.
- Betzler, B.R., Powers, J.J., Brown, N.R., Rearden, B.T., 2017. Implementation of Molten Salt Reactor Tools in SCALE. In: Proc. M&C 2017 - International Conference on Mathematics & Computational Methods Applied to Nuclear Science and Engineering, Jeju, Korea.
- Betzler, B.R., Robertson, S., Davidson, E.E., Powers, J.J., Worrall, A., Dewan, L., Massie, M., 2018. Fuel cycle and neutronic performance of a spectral shift molten salt reactor design. *Ann. Nucl. Energy* 119, 396–410. <https://doi.org/10.1016/j.anucene.2018.04.043>. URL<http://www.sciencedirect.com/science/article/pii/S0306454918302287>.
- Bowman, S.M., 2011. SCALE 6: comprehensive nuclear safety analysis code system. *Nucl. Technol.* 174 (2), 126–148. <https://doi.org/10.13182/NT10-163>. URL<http://pubs.ans.org/?a=11717>.
- Croff, A.G., 1980. User's manual for the ORIGEN2 computer code. Oak Ridge National Lab. Tech. Rep. ORNL/TM-7175.
- Derstine, K.L., 1984. DIF3d: A Code to Solve One-, Two-, and Three-Dimensional Finite-Difference Diffusion Theory Problems. Argonne National Lab. Tech. rep.
- Doligez, X., Heuer, D., Merle-Lucotte, E., Allibert, M., Ghetta, V., 2014. Coupled study of the Molten Salt Fast Reactor core physics and its associated reprocessing unit. *Ann. Nucl. Energy* 64 (Supplement C), 430–440. <https://doi.org/10.1016/j.anucene.2013.09.009>. URL<http://www.sciencedirect.com/science/article/pii/S0306454913004799>.
- Fiorina, C., Aufiero, M., Cammi, A., Franceschini, F., Krepel, J., Luzzi, L., Mikityuk, K., Ricotti, M.E., 2013. Investigation of the MSFR core physics and fuel cycle characteristics. *Prog. Nucl. Energy* 68, 153–168. <https://doi.org/10.1016/j.pnucene.2013.06.006>. URL<http://www.sciencedirect.com/science/article/pii/S0149197013001236>.
- Forget, B., Smith, K., Kumar, S., Rathbun, M., Liang, J., 2018. Integral Full Core Multi-Physics PWR Benchmark with Measured Data. Massachusetts Institute of Technology. Tech. rep.
- Gauld, I.C., Radulescu, G., Ilas, G., Murphy, B.D., Williams, M.L., Wiarda, D., 2011. Isotopic depletion and decay methods and analysis capabilities in SCALE. *Nucl. Technol.* 174 (2), 169–195. <https://doi.org/10.13182/NT11-3>. URL<http://pubs.ans.org/?a=11719>.
- Goluoglu, S., Petrie, L.M., Dunn, M.E., Hollenbach, D.F., Rearden, B.T., 2011. Monte Carlo criticality methods and analysis capabilities in SCALE. *Nucl. Technol.* 174 (2), 214–235. <https://doi.org/10.13182/NT10-124>. URL<http://ans.tandfonline.com/doi/10.13182/NT10-124>.
- Goorley, J.T., James, M.R., Booth, T.E., 2013. MCNP6 User's Manual, Version 1.0, LA-CP-13-00634, Los Alamos National Laboratory.
- Haubenreich, P.N., Engel, J.R., 1970. Experience with the Molten-Salt Reactor Experiment. *Nucl. Technol.* 8 (2), 118–136. <https://doi.org/10.13182/NT8-2-118>.
- Heuer, D., Merle-Lucotte, E., Allibert, M., Doligez, X., Ghetta, V., 2010. Simulation tools and new developments of the molten salt fast reactor. *Revue Générale Nucléaire* (6), 95–100. <https://doi.org/10.1051/rgn/20106095>. URLrgn-publications.sfen.org/articles/rgn/abs/2010/06/rgn20106p95/rgn20106p95.html.
- Heuer, D., Merle-Lucotte, E., Allibert, M., Brovchenko, M., Ghetta, V., Rubiolo, P., 2014. Towards the thorium fuel cycle with molten salt fast reactors. *Ann. Nucl. Energy* 64, 421–429. <https://doi.org/10.1016/j.anucene.2013.08.002>. URL<http://www.sciencedirect.com/science/article/pii/S0306454913004106>.
- Jeong, Y., Choi, S., Lee, D., 2014. Development of Computer Code Packages for Molten Salt Reactor Core Analysis. In: PHYSOR 2014, Kyoto, Japan.
- Jeong, Y., Park, J., Lee, H.C., Lee, D., 2016. Equilibrium core design methods for molten salt breeder reactor based on two-cell model. *J. Nucl. Sci. Technol.* 53 (4), 529–536. <https://doi.org/10.1080/00223131.2015.1062812>. URL<http://www.tandfonline.com/doi/full/10.1080/00223131.2015.1062812>.
- Kee, C.W., McNeese, L.E., 1976. MRPP multiregion processing plant code. Oak Ridge National Lab. Tech. Rep. ORNL/TM-4210.
- LeBlanc, D., 2010. Molten salt reactors: a new beginning for an old idea. *Nucl. Eng. Des.* 240 (6), 1644–1656. <https://doi.org/10.1016/j.nucengdes.2009.12.033>. URL<http://www.sciencedirect.com/science/article/pii/S0029549310000191>.
- Leppanen, J., Pusa, M., Viitanen, T., Valtavirta, V., Kaltainenaho, T., 2015. The Serpent Monte Carlo code: status, development and applications in 2013. *Ann. Nucl. Energy* 82, 142–150. <https://doi.org/10.1016/j.anucene.2014.08.024>. URL<http://www.sciencedirect.com/science/article/pii/S0306454914004095>.
- MCNP – A General Monte Carlo N-Particle Transport Code, 2004. URL<http://mcnp.lanl.gov>.
- Nuttin, A., Heuer, D., Billebaud, A., Brissot, R., Le Brun, C., Liatard, E., Loiseaux, J.M., Mathieu, L., Meplan, O., Merle-Lucotte, E., Nifenecker, H., Perdu, F., David, S., 2005. Potential of thorium molten salt reactors detailed calculations and concept evolution with a view to large scale energy production. *Prog. Nucl. Energy* 46 (1), 77–99. <https://doi.org/10.1016/j.pnucene.2004.11.001>. URL<http://www.sciencedirect.com/science/article/pii/S0149197004000794>.
- O.D. Bank, 2014. The JEFF-3.1.2 Nuclear Data Library, Tech. Rep. JEFF Report 24, OECD/NEA Data Bank.
- Park, J., Jeong, Y., Lee, H.C., Lee, D., 2015. Whole core analysis of molten salt breeder reactor with online fuel reprocessing. *Int. J. Energy Res.* 39 (12), 1673–1680. <https://doi.org/10.1002/er.3371>. URL<http://doi.wiley.com/10.1002/er.3371>.
- Powers, J.J., Harrison, T.J., Gehin, J.C., 2013. A new approach for modeling and analysis of molten salt reactors using SCALE. American Nuclear Society, 555 North Kensington Avenue, La Grange Park, IL 60526 (United States), Sun Valley, ID, USA. URL<https://www.osti.gov/scitech/biblio/2212758>.
- Powers, J.J., Gehin, J.C., Worrall, A., Harrison, T.J., Sunny, E.E., 2014. An inventory analysis of thermal-spectrum thorium-fueled molten salt reactor concepts. In: PHYSOR 2014, JAEA-CONF-2014-003, Kyoto, Japan.
- Robertson, R.C., 1971. Conceptual Design Study of a Single-Fluid Molten-Salt Breeder Reactor. Oak Ridge National Lab., Tenn. Tech. Rep. ORNL-4541, comp, URL<http://www.osti.gov/scitech/biblio/4030941>.
- Ruggieri, J., Tommasi, J., Lebrat, J., Suteau, C., Plisson-Rieunier, D., De Saint Jean, C., Rimpault, G., Sublet, J., 2006. ERANOS 2.1: international code system for GEN IV

- fast reactor analysis. American Nuclear Society, 555 North Kensington Avenue, La Grange Park, IL 60526 (United States). Tech. rep.
- Rykhevskii, A., Lindsay, A., Huff, K.D., 2017a. Online reprocessing simulation for thorium-fueled molten salt breeder reactor. In: Transactions of the American Nuclear Society. American Nuclear Society, Washington, DC, United States.
- Rykhevskii, A., Lindsay, A., Huff, K.D., 2017b. Full-core analysis of thorium-fueled Molten Salt Breeder Reactor using the SERPENT 2 Monte Carlo code. In: Transactions of the American Nuclear Society. American Nuclear Society, Washington, DC, United States.
- Rykhevskii, A., Bae, J.W., Hu, K., 2018. arfc/saltproc: code for online reprocessing simulation of Molten Salt Reactor with external depletion solver SERPENT. <https://doi.org/10.5281/zenodo.1196455>. URL https://zenodo.org/record/1196455#.WrkK_HXwZ9P.
- Scopatz, A., Romano, P.K., Wilson, P.P.H., Huff, K.D., 2012. PyNE: Python for Nuclear Engineering. Transactions of the American Nuclear Society, vol. 107. American Nuclear Society, San Diego, CA, USA.
- Serp, J., Allibert, M., Benes, O., Delpech, S., Feynberg, O., Ghetta, V., Heuer, D., Holcomb, D., Ignatiev, V., Kloosterman, J.L., Luzzi, L., Merle-Lucotte, E., Uhlíř, J., Yoshioka, R., Zhimin, D., 2014. The molten salt reactor (MSR) in generation IV: overview and perspectives. Prog. Nucl. Energy 77 (Supplement C), 308–319. <https://doi.org/10.1016/j.pnucene.2014.02.014>. URL <http://www.sciencedirect.com/science/article/pii/S0149197014000456>.
- Sheu, R.J., Chang, C.H., Chao, C.C., Liu, Y.W.H., 2013. Depletion analysis on long-term operation of the conceptual Molten Salt Actinide Recycler & Transmuter (MOSART) by using a special sequence based on SCALE6/TRITON. Ann. Nucl. Energy 53, 1–8. <https://doi.org/10.1016/j.anucene.2012.10.017>. URL <http://www.sciencedirect.com/science/article/pii/S0306454912004173>.
- T.H. Group, 1997. Hierarchical data format, version 5. <https://www.hdfgroup.org/solutions/hdf5/>.
- U.S. Doe, 2002. A technology roadmap for generation IV nuclear energy systems. In: Nuclear Energy Research Advisory Committee and the Generation IV International Forum, pp. 48–52.
- Xu, Z., Hejzlar, P., 2008. MCODE, Version 2.2: an MCNP-ORIGEN depletion program, Tech. rep., Massachusetts Institute of Technology. Center for Advanced Nuclear Energy Systems. Nuclear Fuel Cycle Program.
- Zhou, S., Yang, W.S., Park, T., Wu, H., 2018. Fuel cycle analysis of molten salt reactors based on coupled neutronics and thermal-hydraulics calculations. Ann. Nucl. Energy 114, 369–383.